J Comp Physiol A (2015) 201:235–248
DOI 10.1007/s00359-014-0965-4

ORIGINAL PAPER

Spider joint hair sensilla: adaptation to proprioreceptive stimulation

Clemens F. Schaber · Friedrich G. Barth

Received: 12 March 2014 / Revised: 23 October 2014 / Accepted: 4 November 2014 / Published online: 15 November 2014

Abstract Adding to previous efforts towards a better understanding of the remarkable diversity of spider mechanosensitive hair sensilla, this study examines hairs of *Cupiennius salei* most likely serving a proprioreceptive function. At the tibia–metatarsus joint of all walking legs, there are two opposing groups of hairs ventrally on the tibia (20 hairs) and metatarsus (75 hairs), respectively. These hairs deflect each other when the joint flexes during locomotion, reversibly interlocking by microtrichs on their hair shafts. The torque resisting the hair deflection into the direction of natural stimulation is smaller by up to two powers of ten than that for the other directions. The torsional restoring constant S of the hair suspension is about 10^{-10} Nm rad^{-1} in the preferred direction, up to a hair deflection angle of 30° (mean of natural deflection angles). Joint movements were imposed in ranges and at rates measured in walking spiders and sensory action potentials recorded. Within the natural step frequencies (0.3–3 Hz) the rate of action potentials follows the velocity of hair deflection. All findings point to the morphological, mechanical, and physiological adaptedness of the joint hair sensilla to their proprioreceptive stimulation during locomotion.

Keywords Mechanosensors · Hair sensilla · Proprioreception · Locomotion · Mechanical directionality

C. F. Schaber (✉)
Functional Morphology and Biomechanics,
Zoological Institute, Kiel University, Am Botanischen Garten 1-9, 24118 Kiel, Germany
e-mail: cschaber@zoologie.uni-kiel.de

C. F. Schaber · F. G. Barth
Department of Neurobiology, University of Vienna,
Althanstraße 14, 1090 Vienna, Austria

Introduction

The coordination of the eight legs of a spider during locomotion requires sensory feedback about the degree of flexion of their joints and the velocities of movement. In the present study, we examine the adaptedness of hair sensilla at the tibia–metatarsus (Ti–Me) joint of the hunting spider *Cupiennius salei* for a proprioreceptive function analyzing their distribution, structure, micromechanical properties, stimulation during walking, and electrophysiological responses.

Each walking leg of an adult spider bears about 150,000 hair sensilla (estimation from hair density and leg surface area) covering a large spectrum of functional types. The most sensitive among them are the trichobothria or filiform hairs. They respond to the frictional forces due to the slightest movements of air (Barth and Höller 1999; Barth 2002, 2004; Humphrey and Barth 2008; McConney et al. 2009). However, the majority of hair sensilla on the leg respond to tactile stimulation. Long exteroreceptive hair sensilla located dorsally on the tarsus and metatarsus were identified as "event detectors" mainly responding to the onset of tactile stimuli (Albert et al. 2001). A single row of proprioreceptive bristles proximally on the leg was found to be adapted to measure the distance between the coxae of neighboring legs (Eckweiler et al. 1989). Groupings of short hair plate sensilla at the joint between coxa and prosoma are proposed to inform the spider about its position in three-dimensional space (Seyfarth et al. 1990). Hair sensilla bridging the metatarsus–tarsus joint respond to substrate vibrations being stimulated by the dorsoventral displacement of the tarsus (Speck-Hergenröder and Barth 1988). Finally, it should also be mentioned that tactile hairs on the sternum elicit reflexes adjusting the distance of the body to the ground of a spider walking over obstacles (Eckweiler and Seyfarth 1988; Seyfarth 2002).

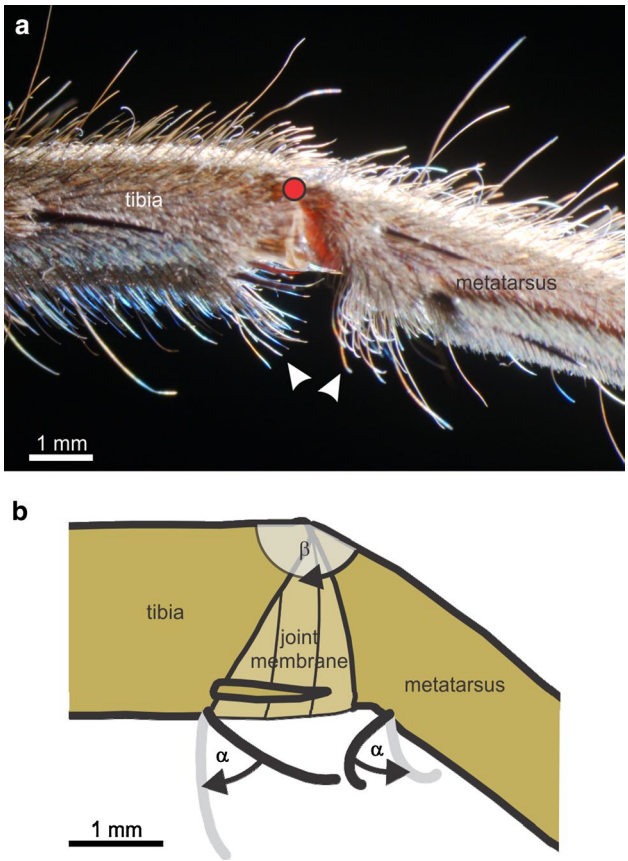

Fig. 1 **a** Photomicrograph of the tibia–metatarsus joint of a second walking leg of *C. salei*; *front view*. The *dot* marks the center of rotation of the joint. The *arrowheads* point to the ventral joint hairs examined in this study. **b** When the joint angle β decreases during joint flexion, the ventral joint hairs of tibia and metatarsus deflect each other from contact onward by the angle α into the direction indicated by the *arrows*. The resting positions of two representative hairs are drawn as thick (not to scale) *black lines* and the maximum deflections indicated in *gray*

To better understand and characterize the diversity of the many thousands of "tactile" hairs found on the spider *C. salei*, here we examine yet another functional type of mechanosensitive hair sensilla. It is found at the Ti–Me joint and likely serves a proprioreceptive function as already proposed by Seyfarth (1985). The Ti–Me joint is of the hinge type with its main plane of movement in the dorsoventral direction and the axis of rotation on the dorsal side (Fig. 1a). To examine whether the sensory hairs at this leg articulation are indeed suited to monitor joint deflection the following aspects were examined: (1) the joint angles and hair deflections during locomotion; (2) the arrangement of the sensory hairs; (3) the hair surface structures leading to reversible coupling to hairs on the opposing leg segments during joint flexion; (4) the mechanical directional characteristics of the suspension of selected hairs; and (5) the potential tuning of the hair's nervous discharges (action potentials) to the natural deflection frequencies occurring during locomotion.

Materials and methods

Animals

All experiments were carried out on adult females of the Central American wandering spider *C. salei* (Keyserling 1877; Barth 2002) bred in the Department of Neurobiology of the University of Vienna. For the measurements of the hairs' deflection during the deflection of the joint, for force measurements, and electrophysiological experiments the animals were briefly anesthetized with CO_2 and tethered onto a holder with adhesive tape. The legs were additionally immobilized with drops of a mixture of colophony and beeswax.

Video analysis

Spiders were filmed in profile (at a right angle to their long axis) during straight runs using a digital video camera (Canon XL 1; Canon Inc., Tokyo, Japan) at 25 frames per second. At the chosen perspective, angular distortions were negligible for the first pair of legs, because *C. salei* moves its Ti–Me joint in parallel to the longitudinal axis of the body. For that reason, all experiments were done with the first pair of legs. Furthermore, the camera's field of view was no more than 15 cm wide so that distortions by the lens itself were negligible. In 54 control experiments with five spiders filmed from above the translational movement of the tibia–metatarsus joint of the first legs was parallel to the longitudinal axis of the body in more than 99 % of the steps.

The animals walked freely in a Perspex gangway (length 60 cm, height 3.5 cm, width 10.5 cm) illuminated by daylight fluorescent tubes. The openings of the gangway at its ends were closed with black cardboard, because *C. salei* orients towards dark objects under light conditions (Schmid 1998). The room temperature during the experiments was 30 °C. The exposure time per frame was set to 1/1,000–1/2,000 s. The recordings were transferred to a PC (Studio DV plus; Pinnacle Systems, Mountain View, CA, USA) and the joint angle β measured frame by frame by marking the dorsal edges of the tibia and metatarsus and the center of the joint's rotational axis (on-screen measurement error 0.38 %, $n = 10$; Software: Videopoint 2.5; Lenox Softworks, Lenox, MA, USA). The mean walking speed was determined from the time taken by the spider's horizontal translational movement and the distance covered between the first and last frame of a recording. Step length was measured at the tip of the tarsus.

Mapping and identification of hairs deflected by joint movements

The hairs deflected by joint movements were observed in living spiders or freshly autotomized legs and documented using a stereomicroscope and a digital camera (Nikon Coolpix 990; Nikon Corporation, Tokyo, Japan). For mapping the topography of the hair sensilla deflected by joint movements under the light microscope, the Ti–Me joint was dissected. A longitudinal cut ventrally in the leg followed by the immersion of the preparation in 5 % KOH solution for about 1 h allowed the tube-shaped leg segments to spread out and flatten. The specimens were dehydrated through a graded concentration series of ethanol and xylene and embedded in Distyrene, a Plasticizer, and Xylene (DPX) mounting medium (Agar Scientific Ltd., Stansted, UK) on microscope slides. To keep the cuticle flat during hardening of the mounting medium, the cover slips were loaded with metal cubes. The outlines of the sockets of the proprioreceptive hairs were drawn using a camera lucida. In order to correlate the shape of their shafts with their position at the joint, individual hairs were plucked out and photographed using a digital laboratory imaging system (Lucia M/Comet 3.52a, Laboratory Imaging s.r.o., Prague, Czech Republic; Camera Sony Power HAD 3CCD, Sony Corporation, Tokyo, Japan on a Laborlux D microscope, Ernst Leitz Wetzlar GmbH, Wetzlar, Germany).

Controlled joint flexion

For the measurement of the angles α of the hair deflections due to joint movements, living spiders were mounted on a metal platform. Hairs not deflected by joint movements were removed. The deflection plane of the hairs of interest was adjusted to the plane of focus of the stereomicroscope with the camera of the digital imaging system. The tibia was fixed with beeswax while the metatarsus was free to be moved using a wire loop. Pictures of the hairs were taken at increasing flexion (decreasing β) of the joint. At a joint angle of $\beta = 180°$ the joint was stretched with the mid-dorsal aspect of tibia and metatarsus forming a straight line. At $\beta < 180°$, the metatarsus was flexed downwards. The deflection angles α of the hair shaft were measured relative to its resting position (Fig. 1b). The measurements were very reproducible (maximum standard error 1.83 % at eight repetitions of the experiment in the same preparation).

Scanning electron microscopy

Ti–Me joints of freshly autotomized legs, kept at an angle β of approximately 135° with small insect pins, were fixed in buffered glutardialdehyde (0.2 M in sodiumcacodylate buffer, 4 % sucrose, pH 7.8) followed by staining with osmium tetroxide (1 %), dehydrated with dimethoxypropane (DMP), pure ethanol and pure acetone, and dried by hexamethyldisilazane (HMDS) evaporation (all chemicals: Sigma-Aldrich Handels GmbH, Wien, Austria). Specimens were sputter coated with gold for 100 s (Model 108; Agar Scientific Ltd., Stansted, UK) and examined in a scanning electron microscope (Philips XL 20; FEI, Eindhoven, The Netherlands) at acceleration voltages of 15–20 kV.

Restoring torques

For the measurement of the restoring moments opposing hair deflection and originating in the hair suspension, the method developed by Dechant (2001), and described in detail in Albert et al. (2001) and Barth et al. (2004), was used. The force opposing hair deflection was measured using the deflection of an individually calibrated glass fiber. The amount of fiber deflection, the relevant lever arm and the degree of a hair's deflection from its unloaded position were quantified using serial digital photographs.

Glass fibers were made from borosilicate glass capillaries (Vitrex; outer diameter 1 mm, inner diameter 0.58 mm, length 100 mm, with filament; Modulohm A/S, Herlev, Denmark) using a laser micropipette puller (Sutter P-2000; settings: heat 600, fil 4, vel 50, del 150, pul 100; Sutter Instruments, Novato, CA, USA). The glass fibers were calibrated at a marked point along their length by bending them in defined steps against a razor blade mounted on a microbalance (Mettler BE 22; Balance Control BA25; Mettler Instrumente AG, Greifensee, Switzerland). Deflection amplitudes measured up to 1 mm. The calibration procedures were controlled optically and carried out on a vibration isolation table (TMC micro g; Technical Manufacturing Corporation, Peabody, MA, USA) in a closed room. The deflection of the glass fiber correlated highly linearly and reproducibly ($R^2 = 0.994$; $n = 15$) with the applied force (0.044 μN μm^{-1}).

The position of single joint hairs was adjusted so that their long axis formed a right angle to the vertically mounted glass fiber at the calibration mark. The hair was then pushed stepwise against the glass fiber and sequences of images were taken and analyzed for hair angle and glass fiber deflection with the image analysis system. The correct position of the calibration mark was controlled optically during the experiments. The torque was calculated as the product of fiber displacement in the image plane and the calibration factor of the glass fiber (force) and the distance of the point where the load was applied on the hair shaft to the hair socket (lever arm).

Electrophysiology

Extracellular action potentials were recorded from single joint hairs with electrolytically sharpened tungsten electrodes. The different measurement electrode was inserted a few

micrometers deep into the cuticle proximally of the sensillum socket using a nanostepper (Scientific Precision Instruments GmbH, Oppenheim, Germany) mounted on a micromanipulator. The grounded indifferent reference electrode was a silver wire inserted into the opisthosoma. For mechanical stimulation a fork made of tungsten wire and mounted on an electrodynamic shaker (Model V101, Ling Dynamic Systems Ltd., Royston, UK) with custom-made feedback control was used (Bohnenberger et al. 1983). The shaker was attached to a micromanipulator on a turntable for the precise adjustment of the deflection stimulus in the plane of natural deflection during walking. The stimulator was driven by an externally triggered function generator (Model 20, Wavetek, San Diego, CA, USA) and the stimulus magnitude adjusted by an attenuator.

Stimuli were either ongoing or single sinusoidal movements presented at intervals of 30 s to simulate a natural stimulus. The interval of 30 s was chosen, because the response intensity to successive single stimuli remained statistically constant, and effects of adaptation could be excluded. At zero point of the sine wave, the stimulator just slightly touched the hair without deflecting it from its resting position. The half sine wave above zero deflected and returned the hair to its initial position in the direction of its natural stimulation. During the half wave below zero, there was no contact between stimulator and hair shaft. The hair deflection amplitude was adjusted optically with an angular grid in the ocular lens of a dissection microscope (Wild M5A, magnification 100×, Wild Leitz Ltd., Heerbrugg, Switzerland). The cross hair of the grid was centered on the pivot point of the hair below its socket, and a deflection by 30° was adjusted with ramp-and-hold deflections. However, although great care was taken to gain the highest precision possible, a reading error by up to 2.2° could not be excluded due to the parallax when measuring the angle with one ocular lens of the stereomicroscope. Different angles could be set by converting the linear voltage output of the stimulator to hair deflection angle.

The recording trace was band pass filtered between 100 and 3,000 Hz, and monitored using a loudspeaker and an oscilloscope. Data were recorded together with the displacement signal of the stimulator via an analog–digital interface (CED 1401, Cambridge Electronic Design Ltd., Cambridge, UK) onto the hard disk of a PC (resolution 10,000 samples s^{-1}). The setup was arranged within a Faraday cage and on a vibration isolation table (TMC micro-g, Technical Manufacturing Corporation, Peabody, MA, USA).

Results

Movement of the joint during locomotion

In freely walking animals the joint angle β reaches a maximum of 174.2° ± 7.6° [mean ± standard deviation (SD), $N = 7$, $n = 41$] when the leg touches down on the ground at the end of the swing phase. Maximum joint flexion and thus the smallest angle β of 119.4° ± 8.6° ($N = 7$, $n = 42$) occur before the leg is lifted from the substrate at the end of the power stroke. Figure 2a shows a representative example of the time-course of the joint angle β at a moderate walking speed of 2 cm s^{-1} of the spider. The mean amount of joint flexion, defined as the difference between the maximum and the following minimum of angle β during one stepping cycle ($\Delta\beta$), is 54.6° ± 8.9° ($N = 7$, $n = 46$). The joint is never flexed to angles of $\beta < 100°$, but frequently extended up to an angle β of approximately 190° (Fig. 2b).

The step duration, which is the time needed for a power stroke (joint flexion) and the following swing phase (joint extension without contacting the substrate), decreases from about 3 s at a walking speed of 1 cm s^{-1} to about 0.8 s at 6 cm s^{-1}. At walking speeds between 6 cm s^{-1} and 20 cm s^{-1} the step duration decreases more slowly down to 0.32 s. Up to a walking speed of 3.5 cm s^{-1}, the flexion and extension phases of the steps decrease simultaneously, whereas at larger velocities the time for joint extension (swing phase) remains fairly constant and only the duration of the stance phase decreases (Fig. 2c). Consequently, the stepping frequency of the first leg pair of *C. salei* during straight forward locomotion under light conditions is 0.3–3 Hz at walking speeds between 1 and 20 cm s^{-1}. Within this range walking speed increases linearly by 6.7 cm s^{-1} Hz^{-1} ($R^2 = 0.94$).

Regarding step length, no clear trend from smaller to larger steps with increasing locomotion velocity of the spider could be seen. Although the smallest step length of 1.6 cm was observed at the slowest speed of 1 cm s^{-1} and the largest step length of 6.4 cm at 12.4 cm s^{-1}, the variability observed was large with a linear regression coefficient R of 0.50 ($N = 7$, 23 runs, $n = 78$ steps). Step widths varied between 1.6 cm and 5.1 cm at walking speeds between 1 and 1.4 cm s^{-1} ($n = 11$), from 2.1 to 5.7 cm at 2.5 to 3.0 cm s^{-1} ($n = 16$), from 3.1 to 5.6 cm at 5.9 cm s^{-1} ($n = 9$), and 4.4 to 5.3 cm at 18.5 cm s^{-1} ($n = 2$), for example.

Distribution and natural deflection of all hair sensilla at the tibia–metatarsus joint

The shape of the joint hair sensilla at the tibia–metatarsus joint and the pattern of their distribution are the same for all of the eight walking legs. Distally on the tibia there are about 310 hair sensilla and on the metatarsus about 400, which are deflected by movements of the joint. The large majority of them are deflected by contact with hairs on the opposing segment of the leg. Only the most distal hairs dorsally on the tibia and the two ventral cuticular spines are deflected by contact with the metatarsal leg cuticle.

The approximately 480 hairs arranged dorsally on the tibia and the metatarsus are deflected only slightly from

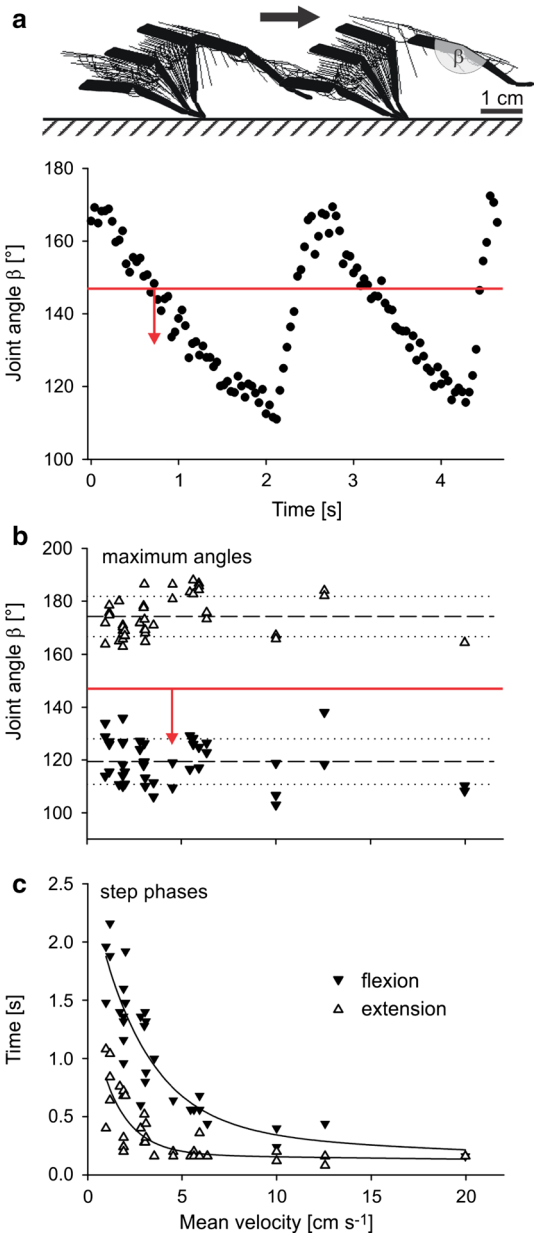

Fig. 2 Movements of the tibia–metatarsus joint during straight forward locomotion. **a** Two steps at a mean walking velocity of 2 cm s^{-1}. The *upper trace* shows the positions of tibia, metatarsus, and tarsus from frame-to-frame video analysis, the *diagram below* the corresponding values of joint angle β. The *red line* indicates the mean threshold angle for the deflection of the ventral joint hair sensilla during joint flexion. **b** Maximum (extension) and minimum (flexion) joint angles β at different walking speeds. The *dashed lines* mark the level of the mean extension and flexion angles, respectively, the *dotted lines* the corresponding standard deviations ($N = 7$, $n = 24$). The *red line* indicates the mean threshold angle for the deflection of the ventral joint hair sensilla during joint flexion. **c** Duration of the joint's flexion and extension phases at different running speeds ($N = 7$, $n = 23$)

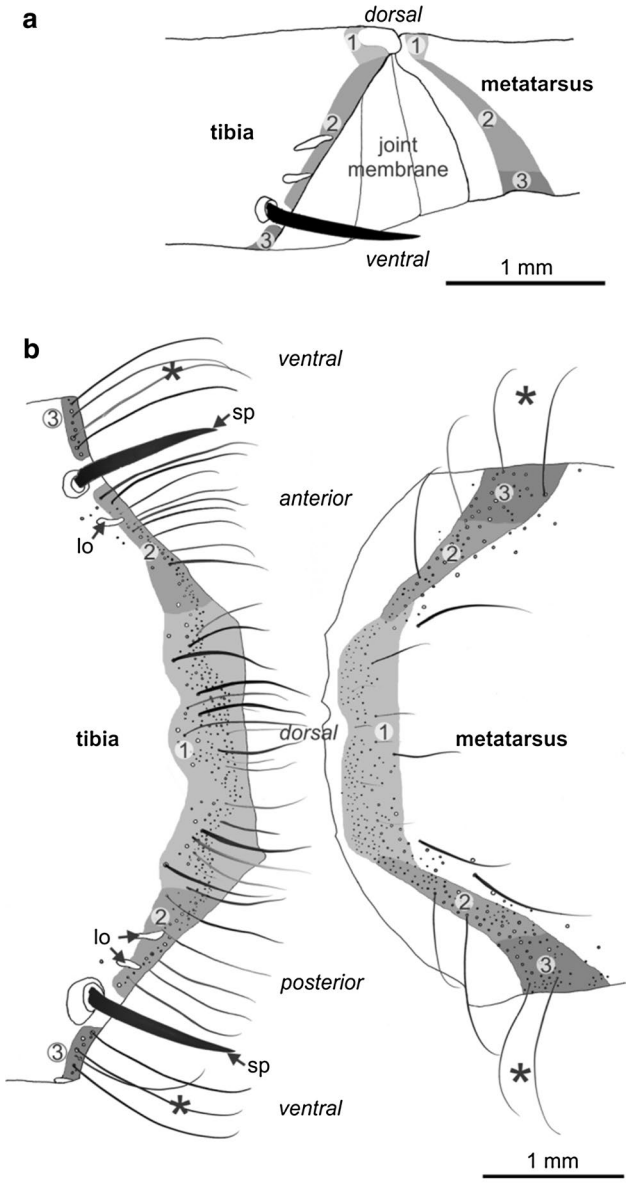

Fig. 3 **a** Posterior view of the joint between tibia and metatarsus. The different areas of joint hairs are indicated by different *shadings* of *gray* and *numbers* referring to the text. **b** Examples of the typical hair shapes in the areas *1–3* (compare with **a**) are drawn in reference to their sockets in a flattened cuticle preparation. *Asterisks* mark joint hairs representing those examined in detail in the present study. The cuticular spines (*sp*) and lyriform organs (*lo*) on the tibia are drawn as landmarks

their resting position and only when the leg is stretched with β being close to 180°. The approximately 230 hair sensilla on the lateral and ventral aspects of the joint are longer than the dorsal ones. They are deflected by up to 60° when the joint is flexed ($\beta < 180°$) during the power stroke.

Six types of putative proprioreceptive hair sensilla can be distinguished by their shape and arrangement pattern and the kind of their natural deflection during joint movement as follows (Fig. 3a, b).

Ti1 hairs on tibia, dorsally: the hair shafts cover the hairless cuticle, which is found directly at and around the joint pans (condyli). Their sockets are arranged in multiple rows

so that several layers of hair shafts bridge the gap to the metatarsus. About 200 such roughly 200–900 µm long hairs are found on the entire dorsal aspect. They are deflected away from the skeletal cuticle by the dorsal metatarsal sensilla when the joint is stretched.

Ti2 hairs on tibia, anterior and posterior: the multiple rows of short hairs dorsally merge to a single row of long hairs ventrally. Anterior-ventrally, there are about 40 hairs between the dorsal edge and the ventral cuticular spine. Their length varies from about 800 µm (most dorsal hairs) to 1,600 µm (most ventral ones). About 50 hairs are arranged posterior-ventrally in a way similar to that of the hairs on the anterior-ventral aspect. Their lengths vary between 700 and 1,500 µm.

Ti3 hairs on tibia, ventrally: between the two large cuticular spines are 20 ± 4 ($N = 20$) joint hair sensilla, which form a single row at the edge of the sclerotized cuticle to the joint membrane. The sockets of these hairs are about 50 µm away from the "normal" hair coat of the tibia. Their shafts are 1,400 ± 200 µm ($N = 8$, $n = 32$) long and deflected away from the joint membrane by type Me3 hairs of the metatarsus (Figs. 1b, 3b).

Me1 hairs on metatarsus, dorsally: about 280 approximately 130–500 µm long sensilla are arranged in multiple rows. The hair tips point distally with regard to the leg and the hair shafts form a small angle with the leg cuticle surface. The angle and the length of these hairs increase with their distance from the joint. When the joint is stretched, they are pushed down slightly by the dorsal sensilla of the tibia.

Me2 and Me3 hairs on metatarsus, ventrally: about 120 proprioreceptively deflected sensilla are arranged on the ventral aspect of the metatarsus, starting below the joint sockets of the metatarsus at the Ti–Me joint. Here the basal parts of the hair shafts form roughly a right angle (88° ± 12°; $N = 6$, $n = 18$) with the exoskeletal surface and the hair tips are bent pointing towards the leg tip. Their lengths vary between roughly 700 and 1,200 µm. During joint flexion the Me2 and Me3 hairs are deflected by the Ti2 and Ti3 hairs opposing them on the anterior, posterior and ventral aspect of the tibia. The Ti3 and the Me3 hairs and their interaction during joint flexion are examined in detail within this study.

The two hydraulically erectile spines on the tibia are innervated as well (Harris and Mill 1977; Foelix 1996). They are shorter (about 1,200 µm) than the hairs surrounding them and deflected only by direct contact with the exoskeletal cuticle of the metatarsus at large joint flexions with angles β smaller than roughly 135°.

Mechanical threshold and natural deflection of the ventral joint hairs

The mechanical threshold of hair deflection is indicated by the onset of hair shaft movement due to the flexion of the joint. Of the ventral Ti3 hair sensilla the deflection threshold is at a joint angle β of 147° ± 10° ($N = 8$, $n = 32$). A similar value is found for the neighboring Ti2 sensilla at 148° ± 19° ($N = 4$, $n = 25$) anteriorly on the tibia and 147° ± 7° ($N = 4$, $n = 16$) posteriorly on the tibia. Together they form a functional entity of approximately 110 hair sensilla, which are simultaneously deflected during joint flexions at angles of $\beta \leq 147°$, which occur at every step of the walking spider (Fig. 2b), by roughly 120 opposing Me2 and Me3 sensilla.

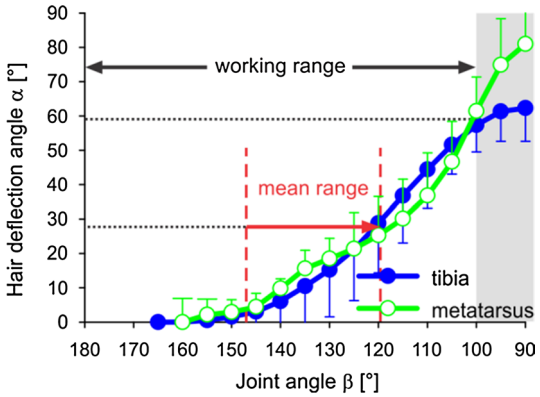

Fig. 4 Mean deflection α (±SD) of Ti3 ($N = 8$, $n = 32$) and Me3 ($N = 6$, $n = 18$, each measured six times) joint hairs as a function of joint angle β (bin width 5°). Joint angles β within the *shaded area* (<100°) are not reached during active locomotion of the spider; note inverted scale of *x*-axis

During locomotion joint flexions down to a joint angle β of 100° occur. Within this range, the mean deflection curves of the Ti3 and Me3 joint hairs, which are examined in more detail in the present study, are very similar with maximum hair deflection angles α of approximately 60°. Within the mean working range, joint flexion amplitudes go down to angles β of approximately 120° (Fig. 2b), and the ventral joint hairs of both the tibia and the metatarsus deflect each other by as much as $\alpha = 30°$ (Fig. 4).

Functional morphology of the hair shafts and sockets

The shafts of the Ti3 and Me3 hairs are covered with tens of thousands of cuticular protuberances (microtrichs). Their density varies with the length and diameter of the hair shaft. The microtrichs emerge from ripples parallel to the long axis of the hair shaft starting from 25 µm above the suspension of the hair in the cuticle up to the hair tip. They form regular rows with a distance of 1 µm between them. Dependent on the hair shaft's cross section there are from 15 microtrichs per µm of hair length in the tip region, and up to 25 microtrichs per µm in the basal region of the hair shaft. The microtrichs are cone shaped, 5 µm long, and about 1 µm thick at their base. Their tips are 150 nm wide and seem to form a small hook. When the Ti3 and Me3 hairs

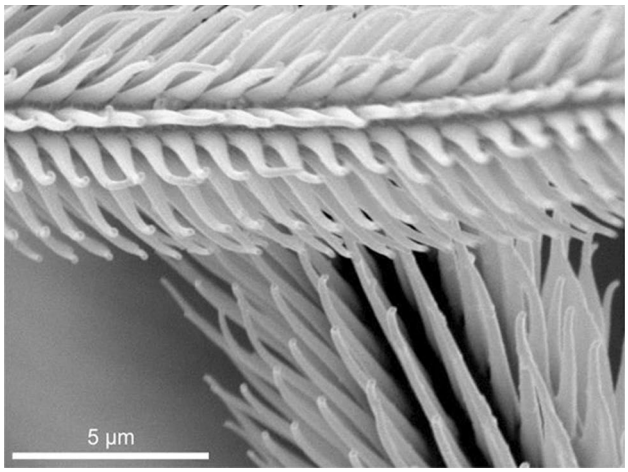

Fig. 5 Microtrichs on the hair shaft of a Ti3 (*top*) and a Me3 hair (*below*) in contact with each other at a joint angle β of 135°. Microtrichs interlock slightly

are in contact during flexion of the leg joint, the contact area is limited to the tip region of the microtrichs (Fig. 5). Thus, the two joint hairs deflect one another while they are loosely and reversibly interlocked by their microtrichs.

Viewed from above the sockets of the Ti3 hairs are nearly circular. In the non-deflected state, the membrane of the hair suspension bulges outward between the basal hair shaft and the socket wall at the side of natural deflection during walking. Here the distance between the hair shaft and the socket wall is much larger than in the other possible directions of hair deflection (Fig. 6a, b). When viewed from above the socket of the Me3 hairs is slightly elliptic with its longer diameter in the plane of the hair shaft's movement during walking. The wall formed by the hair socket is lower in the direction of hair deflection under natural stimulation compared to the other sides (Fig. 6b). All these structural characteristics facilitate large angle deflections of the hairs in the relevant direction.

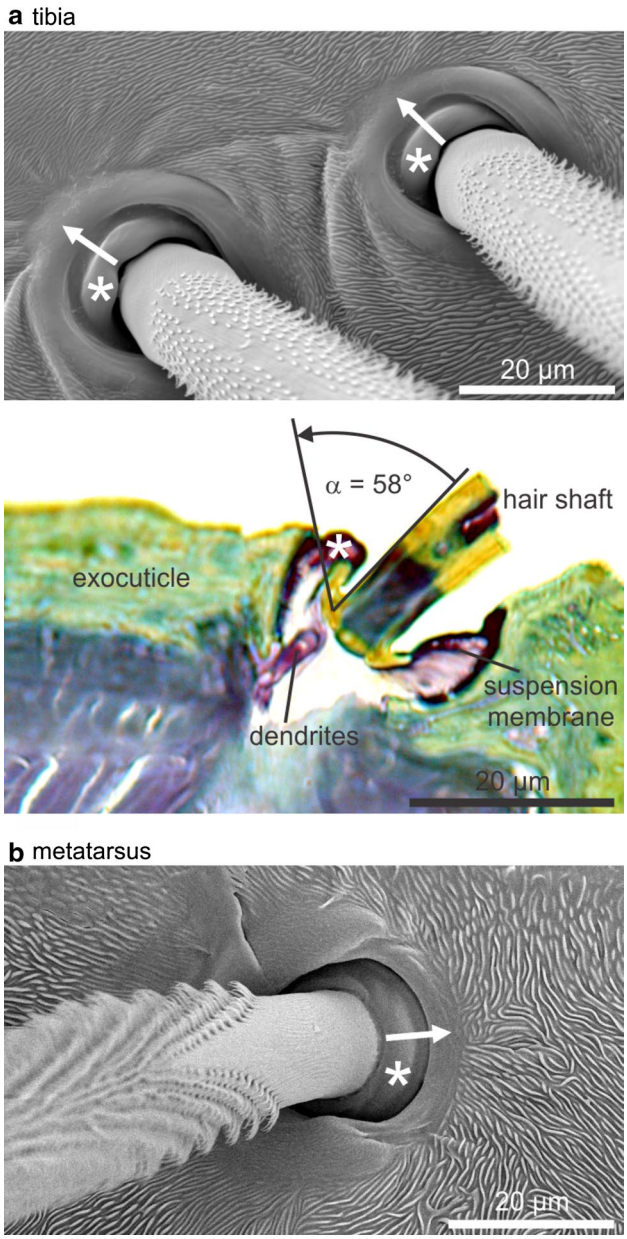

Fig. 6 Hair sockets of the ventral joint hairs. *Arrows* indicate the directions of natural deflection during walking. **a** SEM micrograph of two sockets of Ti3 hairs. *Below* a photomicrograph of a semi-thin section of a hair socket. Toluidine blue stained (slice by courtesy of R. Müllan). *Asterisks* indicate the bulging joint membrane. The hair shaft rotating in the natural direction (*arrow*) contacts the stiff exocuticle at an angle of 58°. **b** Socket of a Me3 hair

Mechanical directionality

The restoring torques of the Ti3 sensilla located ventrally of the posterior cuticular spine and those on the metatarsus opposing them (Me3) were measured (Fig. 3b). Six consecutive deflections of the hair shaft in four directions (proximad, distad, anteriad, posteriad) were examined in each preparation and the torques applied plotted as a function of the hair deflection angle α (Fig. 7a).

At $\alpha \leq 50°$ in the direction of natural stimulation during walking the torques rise slowly from zero to about 1 nN m in both the tibial and the metatarsal sensilla. At angles of $\alpha > 50°$ the significant increase of the torques needed to further deflect the hairs indicates the increasing contact of the basal hair shaft with the socket walls and therefore its bending (Fig. 6a). When the hair shafts are deflected into the other directions (i.e., opposite, anteriad, and posteriad) the torque values increase much more quickly with deflection angle, the greatest resistance being in the direction opposite to the natural one (Fig. 7a). The iso-torque plots shown in Fig. 7b clearly demonstrate the pronounced directional characteristics of the hair suspensions.

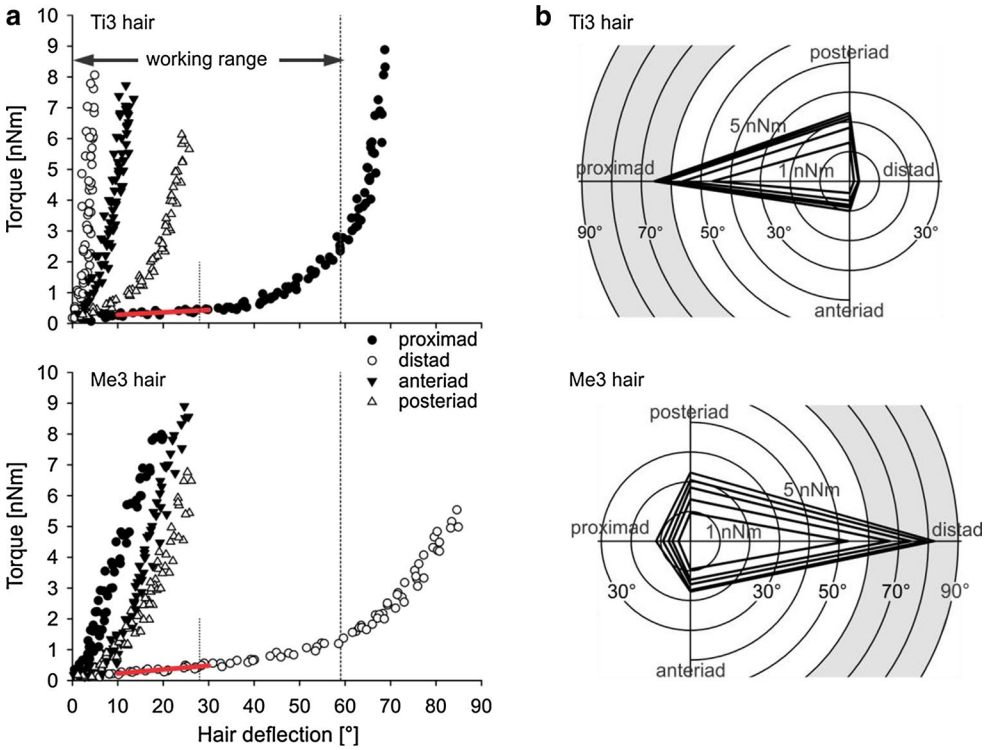

Fig. 7 Mechanical directionality of the joint hairs. **a** Torques at deflections of a Ti3 hair into four different directions defined according to the leg's long axis (proximad-distad). The *dotted vertical line* at 59° marks the maximum hair deflection by joint flexion during locomotion; the *line* at 28° marks the mean value of hair deflection during locomotion (compare Fig. 4). The *regression line* (*red*) was used to determine the torsional restoring constant *S*. Below is the corresponding graph for a Me3 hair. **b** Polar plots of the torques. The iso-torque lines connect the mean angles of deflection ($n = 6$) required to reach torques ranging from 1 (*innermost line*) to 5 nN m (*outermost line*). Angles within the *shaded area* do not occur during locomotion

Table 1 Parameters (mean values) and correlation coefficients R^2 of the exponential function $T = T_0 + ae^{b\alpha}$ (Nm × 10^{-9}) fitted to the measured torque values T (six preparations and hairs each)

	T_0	a	b	R^2
Tibia hairs				
Proximad[a]	0.37 ± 0.08	0.001 ± 0.001	1.17 ± 0.02	0.96 ± 0.02
Distad	−3.55 ± 4.43	3.59 ± 4.45	0.22 ± 0.22	0.86 ± 0.08
Anteriad	−4.60 ± 4.42	4.15 ± 4.21	0.09 ± 0.04	0.92 ± 0.05
Posteriad	−0.50 ± 0.86	0.63 ± 0.72	0.12 ± 0.05	0.96 ± 0.02
Metatarsus hairs				
Proximad	−6.63 ± 10.46	6.38 ± 10.49	0.08 ± 0.06	0.91 ± 0.05
Distad[a]	0.12 ± 0.18	0.07 ± 0.08	0.06 ± 0.03	0.98 ± 0.01
Anteriad	−3.42 ± 3.06	3.19 ± 2.85	0.06 ± 0.04	0.96 ± 0.02
Posteriad	−3.38 ± 4.01	3.25 ± 3.88	0.05 ± 0.04	0.96 ± 0.02

T_0 is the extrapolated value of T at a hair deflection angle of 0°. a and b are constants, and R^2 is the correlation coefficient of the fitted curve with the experimental data

[a] Natural direction during walking

The increase of the torque T with deflection angle α can be well described ($R^2 > 0.85$) for all directions tested by the exponential function $T = T_0 + ae^{b\alpha}$, where T_0, a and b are constants (Table 1).

Torsional restoring constants *S*

In the direction of stimulation during walking the torsional restoring constant S of the hair suspension can be evaluated from the linear region of the torque curve between $\alpha = 10°$ and $\alpha = 30°$ (Fig. 7a). The values of S of the Ti3 hairs are between 5.0 × 10^{-12} and 2.3 × 10^{-11} Nm deg^{-1}, and 2.9 × 10^{-10} and 1.3 × 10^{-9} Nm rad^{-1}, respectively ($N = 6$). The torsional restoring constants of the Me3 hairs are similar and measure between 5.4 × 10^{-12} and 1.7 × 10^{-11} Nm deg^{-1}, and 3.1 × 10^{-10} and 1.6 × 10^{-9} Nm rad^{-1}, respectively ($N = 6$) (Table 2). Within this linear range, the restoring torques can be related to the extension of a linear spring element within the hair suspension. Consequently, because of the similarity of the

Table 2 Elastic restoring constant *S* of the joint hairs as derived from torque measurements in the linear range of the torque-deflection function (six preparations and hairs each)

	Mean (Nm rad^{-1})	SD (Nm rad^{-1})	Minimum (Nm rad^{-1})	Maximum (Nm rad^{-1})
Tibia hairs				
Proximad[a]	5.92×10^{-10}	3.85×10^{-10}	2.86×10^{-10}	1.33×10^{-9}
Distad	3.69×10^{-8}	2.64×10^{-8}	5.40×10^{-9}	8.02×10^{-8}
Anteriad	2.17×10^{-8}	1.34×10^{-8}	8.10×10^{-9}	3.93×10^{-8}
Posteriad	6.90×10^{-9}	2.69×10^{-9}	4.22×10^{-9}	1.10×10^{-8}
Metatarsus hairs				
Proximad	1.51×10^{-8}	1.05×10^{-8}	3.59×10^{-9}	2.86×10^{-8}
Distad[a]	8.03×10^{-10}	4.54×10^{-10}	3.09×10^{-10}	1.60×10^{-9}
Anteriad	1.50×10^{-8}	9.29×10^{-9}	4.85×10^{-9}	2.74×10^{-8}
Posteriad	6.19×10^{-9}	3.70×10^{-9}	2.04×10^{-9}	1.21×10^{-8}

[a] Natural direction during walking

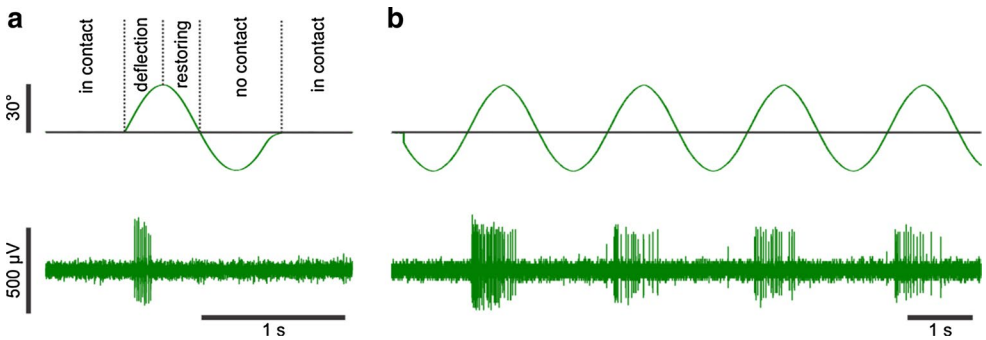

Fig. 8 Action potentials (*lower trace*) of a Ti3 hair sensillum elicited by simulated stepping patterns (*upper trace*). **a** Single step corresponding to a step duration of 1 s and a stepping rate of 1 Hz. Marked are the different phases of hair deflection. **b** Four steps of ongoing stimulation at a stepping rate of 0.5 Hz and a step duration of 2 s. The phases of hair deflection are the same as in **a**

S values of the tibia and metatarsus hair suspensions, both hair types are deflected by roughly the same amount when the joint is flexed during locomotion.

The stiffness of the hair suspension is larger in the other directions. The values of *S* listed in Table 2 were derived from the quasi-linear rise of the torque curves at deflection angles $5° < \alpha < 30°$. Compared to deflections in the proximad direction, the stiffness of the Ti3 hair suspension is 62-times larger in the distad direction of deflection, 37-times in the anteriad, and 12-times in the posteriad direction. For the Me3 hairs the mechanical directional characteristics are slightly less pronounced. As compared to the distad deflection, a 19-fold larger stiffness towards the proximal and anterior direction and eightfold stiffness for posteriad deflections were found.

Electrophysiological response properties

To approximate the natural stimulus pattern, sinusoidal half wave deflections of different frequencies with angles of $\alpha = 30°$ were applied to single joint hair sensilla of types Ti3 and Me3 in the direction of movement during joint flexion. This quasi-natural stimulus pattern roughly corresponds to the joint flexion pattern during locomotion with β varying between 150° and 120°.

Only the deflection of the hairs away from their resting positions elicits rapidly adapting bursts of action potentials set off following the start of the movement. No action potentials are generated during the return of the hairs to their resting positions (Fig. 8a). With ongoing stimulation, the response pattern is similar to that for single steps. However, the decrease of number and rate of action potentials with the number of simulated steps point to a certain adaptation of the sensor (Fig. 8b). In order to exclude the effects of adaptation from statistical analysis, the results of single-step simulations with an adequate time interval in between two stimulations were further analyzed.

The mean frequency of action potentials, calculated from the time between the first and the last impulse divided by the number of impulses during one burst, follows the stepping rate closely and consequently the velocity of hair deflection up to the natural limit of 3 Hz, and an initial hair deflection velocity of 520° s^{-1}, and 9.1 rad s^{-1}, respectively. At deflection velocities exceeding the natural range, the increase of the rate of action potentials is less pronounced. This trend can be seen in the results of all experiments with six repetitions at each simulated stepping rate, and in both the Ti3 and the Me3 hairs (Fig. 9a). The same trend could be found when the maximum frequencies

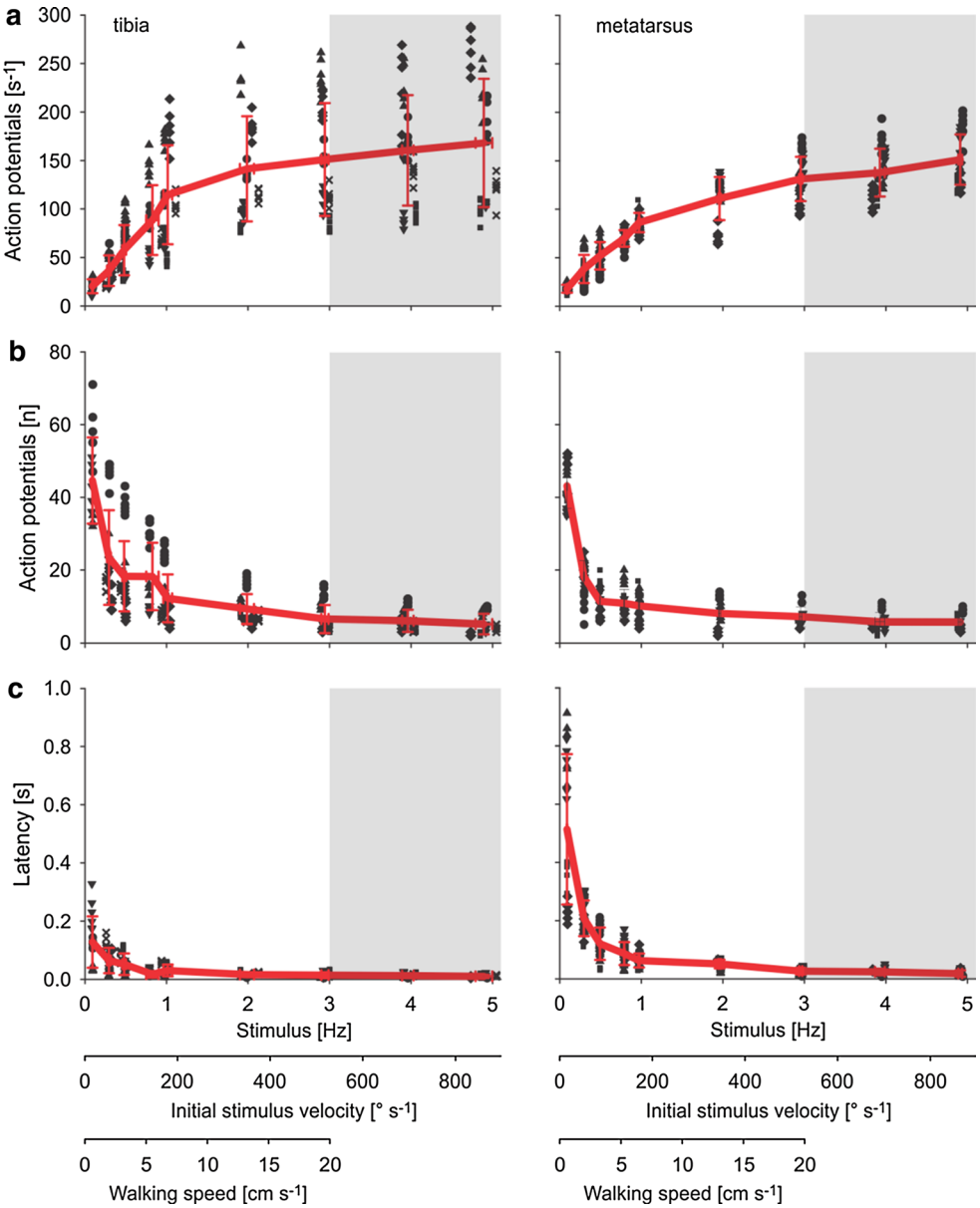

Fig. 9 Sensory response (action potentials) of the ventral joint hair sensilla to deflections by $\alpha = 30°$ by stimulation with sinusoidal half waves in the direction of natural stimulation during walking. Ti3 hairs on the *left* and Me3 hairs on the *right*. The *filled symbols* are original data. The *lines* connect the mean values (±SD) of six Ti3 ($N = 6$, $n = 36$), and five Me3 ($N = 5$, $n = 30$) hairs, respectively. Stimulus velocities within the *shaded* area are not reached during locomotion of the spider. **a** Mean rate of action potentials during the response. **b** Number of action potentials during the response. **c** Latency of the first action potential to the onset of the stimulus

of action potentials, the inverse of the minimum time interval between two action potentials during one burst, were evaluated.

The deflection of the hairs away from their resting position elicits bursts of up to 50 action potentials at the slowest simulated stepping rate of 0.1 Hz, corresponding to one step per 10 s. The number of action potentials decreases quickly with increasing stimulus velocity down to 5 at a simulated stepping rate of 5 Hz (Fig. 9b).

The latency of the sensory response, which was measured as the time interval between the onset of hair deflection and the first action potential, decreases quickly from a mean value of 128 ms at stimulus velocities of 17° s^{-1} (0.1 Hz) down to a mean value of 30 ms at 177° s^{-1} (1 Hz) in Ti3 hairs, and from 514 ms down to 63 ms in Me3 hairs, respectively. The latency values remain small at higher stimulus velocities and decrease slightly to 14 ms at 521° s^{-1} (3 Hz) and 10 ms at 883° s^{-1} (5 Hz) in Ti3 hairs, and 26 and 18 ms in Me3 hairs, respectively (Fig. 9c).

The angular deflection threshold necessary to elicit one action potential with quasi-natural sinusoidal stimulation was $\alpha = 7.3° \pm 4.2°$ at simulated step frequencies tested up to 10 Hz ($N = 4$, $n = 43$), and varied between 0.7° and 15°. No trend could be seen regarding a decrease or increase of the angular threshold deflection towards larger stimulus rates, and deflection velocities, respectively.

At linear ramp-and-hold deflections with a constant hair deflection velocity of 40° s^{-1} towards final angles between $\alpha = 6°$ (threshold angle of the preparation) and $\alpha = 30°$ the action potential frequency of the sensory response remains

the same. In the same angular range, the total number of action potentials increases from 100 to about 250, which is thought to be mainly due to the longer duration of the dynamic stimulus phase of the hair movement. No action potentials are generated during static deflection of the hairs.

Discussion

Pattern of hair arrangement

During locomotion, a multitude of hair sensilla at the tibia–metatarsus joint of *C. salei* is stimulated due to their pattern of arrangement and shape. The tips of the Ti2 and Ti3 hairs roughly form a straight line (Fig. 3), representing a sensory collar consisting of approximately 110 hairs. These are initially stimulated when their tips contact approximately 120 Me2 and Me3 hairs at a joint angle β of about 150°. At smaller angles of β, all these hair sensilla deflect each other, being reversibly interlocked by their microtrichs (Fig. 5) and stimulated in synchrony with the spider's stepping pattern. The dorsal Ti1 and Me1 sensilla (Fig. 3) may be stimulated when the leg is fully extended (i.e., $\beta \approx 180°$), but no physiological data are available yet for this situation.

Locomotion and micromechanics of hair deflection

Flexion of the tibia–metatarsus joint during locomotion typically leads to a deflection of both the Ti3 and the Me3 hairs to angles of $\alpha \approx 30°$ (Fig. 4). The microtrichs on the hair shafts (Fig. 5) are suggested to enhance the friction between two interacting hairs of the two leg segments and ensure contact during hair deflection.

The torque needed to deflect a joint hair in its mechanically preferred proprioreceptive direction is well below 1 nN m for angles of $\alpha \leq 30°$. From $30° \leq \alpha \leq 60°$ the resistance to deflection increases non-linearly. At $\alpha > 60°$ the torque values rise steeply and reach values of 9 nN m at $\alpha = 70°$ (Fig. 7), because the hair shaft is contacting the socket wall and bent. At deflection angles below 30°, the hair shaft behaves like a stiff rod rotating around the pivot point inside the hair suspension structures. Likely, between 30° and approximately 60°, the hair suspension material located between the hair shaft and the socket wall is more and more compressed, leading to the non-linear increase of the torques (Figs. 6a, 7). Interestingly, the steep increase of torque at a hair deflection angle of $\alpha = 60°$ coincides with a joint angle of $\beta = 100°$ and represents maximum hair deflection at maximum joint flexion during locomotion. Hence, the hair socket structures obviously are well adapted to deal with the deflections of the hair shaft actually occurring during locomotion.

The slightly softer suspension of the metatarsal hairs as compared to that of the tibia hairs in the direction of natural stimulation is due to the lack of the elevated socket wall at the corresponding side (Fig. 6). This implies that the shafts of the metatarsal hairs contact their socket walls at larger deflection angles than the tibia hairs as indicated by the lower torque values (Fig. 7).

A similar structural arrangement may account for the larger stiffness of the suspension of both the Ti and Me hairs in directions other than the natural one. In their resting position the hair shafts are closer to the socket walls in these other directions, contacting them at smaller deflection angles, and thus leading both to the earlier rise of the curves shown in Fig. 7 and to larger torques.

Although the exponential dependence of the torque T on the hair deflection angle α has not been extensively analyzed, one might argue that the increasing resistance of the suspension and the bending of the hair shaft together are the main parameters determining this mechanical behavior.

Signaling the velocity of joint flexion

The results of the electrophysiological part of this study are even more substantial, if one considers that more than 100 hairs on tibia and metatarsus are deflected synchronously when the joint is flexed during locomotion. The joint hair sensilla are pure movement detectors as no action potentials are set off during static deflection and in the resting position. The sensilla monitor the flexion of the Ti–Me joint at joint angles β below about 150° for every step of the spider (Figs. 2b, 8). The velocity of joint flexion, especially at low stimulus velocities, and step rates, respectively, is well resolved by the rate of action potentials. The response magnitude saturates at step rates exceeding the natural stimulus range during walking (Figs. 2c, 9a). Therefore, the joint hair sensilla could serve as feedback sensors for fine control of the joint movement during walking and slow joint flexions as they occur, for example, when weaving a cocoon.

During walking the step frequency can be detected by the bursts of action potentials triggered by every step of the spider (Fig. 8b). For that purpose the signaling of the start of hair deflection is sufficient. Fast joint flexions when grabbing prey with velocities in the saturation range of the joint hair sensilla are registered as well with small latency times (Fig. 9c).

The highly linear increase of locomotion velocity with stepping frequency and the larger impact of joint flexion than extension time on step duration (Fig. 2c) point to joint flexion velocity being the most important factor for the walking speed of the spider. The scatter of 20° of both the minimum and the maximum of Ti–Me joint flexion angle β (Fig. 2b) is reflected by the large variation of step lengths at the different walking speeds.

Comparison with other hair-shaped sensilla of *Cupiennius salei*

The findings on the functionality of the joint hairs add to the detailed understanding of different functional types of mechanoreceptive hair sensilla of *Cupiennius*. To date, the mechanical and physiological properties are known in some detail for the airflow sensing trichobothria and the long tactile hair sensilla on the tarsi and metatarsi only. In both cases, the mechanical properties of the hair suspension reflect strikingly different movabilities of the hair shaft and differences in function (Barth 2004).

The tactile hair sensilla studied on the tarsus and metatarsus are stimulated by direct contact with solid substrate (Albert et al. 2001). Their mechanical directional characteristics are nearly isotropic and their socket walls higher than that of the joint hairs and without an "opening" leading to a mechanically preferred direction of hair deflection. The torque of the tactile sensilla resisting their deflection rises exponentially to 1 nN m at a deflection angle of $\alpha \approx 7°$ and to 5 nN m at $\alpha \approx 15°$. These values are similar to those of the joint hair sensilla when deflected into directions other than that during natural stimulation. When deflected, the hair shaft of the tactile hairs is not only bent when it touches the rim of its cuticular socket, but also bends inside the socket at even smaller deflections protecting it from breakage (Barth et al. 2004). In the joint hair sensilla, bending of the hair shaft during proprioreceptive large angle deflections is thought to be minimized by the distance of the hair shaft from the hair socket (Fig. 6).

The restoring constant S of the tactile hairs amounts to 3×10^{-8} Nm rad^{-1} (Albert et al. 2001). This value is again well within the range of those found for the joint hair sensilla for deflections into directions other than the one occurring naturally during locomotion (2.04×10^{-9} –8.02×10^{-8} Nm rad^{-1}). However, it is larger by one to two orders of magnitude than S measured for the joint hair sensilla when deflecting them in the biologically relevant, proprioreceptive direction (2.86×10^{-10} –1.60×10^{-9} Nm rad^{-1}). Compared to the suspension stiffness of the air flow sensing trichobothria, where the S values are as small as 4.30×10^{-12}–6.2×10^{-11} Nm rad^{-1} (Barth et al. 1993; McConney et al. 2009), the resistance of the joint hair sensilla even to deflections in the proprioreceptive direction is larger by two orders of magnitude.

Trichobothria generate one action potential when deflected by only 0.01°–0.1°, which renders them extremely sensitive for the slightest movements of the air. With a threshold angle of 1°, the tactile hairs are well suited as detectors for rapid touch events. In the joint hair sensilla, the threshold angle of about 7° is comparatively large. It may help to filter out stimuli by smaller movements of the substrate irrelevant for sensing the joint's flexion velocity during the stance phase of walking.

Comparison with proprioreceptive hair sensilla of other arthropods

Proprioreceptive hair sensilla involved in sensing movement and position of joints are found at many different joints and in many arthropod species. Many of them are arranged as hair plates or hair rows and deflected by contact with joint membranes or solid cuticle. The number of deflected hairs of a hair plate and the intensity of the sensory response often correlates with joint angle. Whereas the type of response of all hairs of the coxal hair plates of *Cupiennius* is slowly adapting, the hairs differ in being responsible for a particular region of possible joint angles (Seyfarth et al. 1990). In insects and crustaceans, usually both phasic and tonic and/or phasic-tonic (slowly adapting) units are found coding for joint deflection velocity and joint position, respectively. A few examples shall illustrate this.

Hair plate sensilla of the praying mantis *Tenodera sinensis* monitor head motion and are involved in the measurement of prey distance (Poteser et al. 1998). The hair plates at the neck of black soldier flies *Hermetia illucens* are directionally sensitive and respond to head movements as well (with excitation or inhibition) (Paulk and Gilbert 2006). On the stinging apparatus of the honeybee *Apis mellifera* rows of up to 30 very short (14–24 µm) hair sensilla respond to the protraction of the lancet, and are supposed to detect its position relative to the stylet during stinging (Ogawa et al. 2011). In the rock lobster *Palinurus vulgaris* a hair plate of some 118 slowly adapting sensilla at the basal antenna joint signals the velocity of antennal movement and presumably also joint position by the number of excited hairs (Vedel 1986). There is some detailed information on coxal and tibial hair plates in the locust *Schistocerca gregaria* and their involvement in locomotion (Kuenzi and Burrows 1995; Newland et al. 1995). The same applies to the stick insect *Carausius morosus* (Wendler 1964; Bässler 1977; Dean and Schmitz 1992), and data on the stimulation of joint hairs and hair plate sensilla are also available for the cockroach *Periplaneta americana* (Pringle 1938; Wong and Pearson 1976; French and Wong 1976).

Sensory information from different joint receptor types

Besides hair sensilla like those described in the present study there are multiterminal neurons with dendrites ending beneath the articular membranes and sensing the angular position of spider leg joints (Foelix and Choms 1979). The theraphosid spider *Eurypelma hentzi* has many tonic units among these receptors at the femur–patella joint, which respond to changes of the joint angle by altering

their stationary impulse frequency (Rathmayer 1967). Similar findings are reported for the tibia–metatarsus joint of the meshweb weaver *Amaurobius* (=*Ciniflo*; Mill and Harris 1977).

In addition to the hair sensilla examined in the present study and two dorsolateral groups of internal joint receptors (Seyfarth and Pflüger 1984), the tibia–metatarsus joint of *C. salei* is equipped with four lyriform organs distally on the tibia, which respond to cuticular strains generated during locomotion (Blickhan and Barth 1985). The axons of the sensory cells of the internal receptors and of the lyriform organs go together with those of the hair sensilla at the joint (Seyfarth and Pflüger 1984).

Seyfarth (review 2002) showed an interesting interplay of tactile hairs and internal joint receptors leading to body raising behavior when the spider walks over an obstacle. The stimulation of tactile hairs proximally on the ventral side of a leg first elicits muscle contractions in the stimulated leg only. As a consequence, internal joint receptors at the same leg's prosoma–coxa joint are activated, which finally induces a plurisegmental reaction by muscle contractions in all eight legs mediated by identified plurisegmental interneurons.

The quick return to the normal movement pattern following preliminary ablation experiments with the joint hairs points to a redundancy of the sensory systems controlling locomotion. Apart from joint hairs, the spider has slit sensilla on the leg segments (Barth and Libera 1970), in particular the lyriform organs close to the joints (Blickhan and Barth 1985; Schaber et al. 2012), and internal joint receptors (Seyfarth and Pflüger 1984).

Acknowledgments Partially supported by a grant of the Austrian Science Fund (FWF, P12192-BIO) to F.G.B. The experiments comply with the Principles of Animal Care and the current laws of Austria where they were carried out.

References

Albert JT, Friedrich OC, Dechant H-E, Barth FG (2001) Arthropod touch reception: spider hair sensilla as rapid touch detectors. J Comp Physiol A 187:303–312

Barth FG (2002) A spider's world: senses and behavior. Springer, Berlin

Barth FG (2004) Spider mechanoreceptors. Curr Opin Neurobiol 14:415–422

Barth FG, Höller A (1999) Dynamics of arthropod filiform hairs. V. The response of spider trichobothria to natural stimuli. Philos Trans R Soc Lond B 354:183–192

Barth FG, Libera W (1970) Ein Atlas der Spaltsinnesorgane von *Cupiennius salei* Keys. Chelicerata (Araneae). Z Morphol Tiere 68:343–369

Barth FG, Wastl U, Humphrey JAC, Devarakonda R (1993) Dynamics of arthropod filiform hairs. II. Mechanical properties of spider trichobothria (*Cupiennius salei* Keys.). Phil Trans R Soc Lond B 340:445–461

Barth FG, Németh SS, Friedrich OC (2004) Arthropod touch reception: structure and mechanics of the basal part of a tactile hair. J Comp Physiol A 190:523–530

Bässler U (1977) Sensory control of leg movement in the stick insect *Carausius morosus*. Biol Cybern 25:61–72

Blickhan R, Barth FG (1985) Strains in the exoskeleton of spiders. J Comp Physiol A 157:115–147

Bohnenberger J, Seyfarth E-A, Barth FG (1983) A versatile feedback controller for electro-mechanical stimulation devices. J Neurosci Methods 9:335–341

Dean J, Schmitz J (1992) The two groups of sensilla in the ventral coxal hairplate of *Carausius morosus* have different roles during walking. Physiol Entomol 17:331–341

Dechant H-E (2001) Mechanical properties and finite element simulation of spider tactile hairs. Doctoral thesis, Vienna University of Technology

Eckweiler W, Seyfarth E-A (1988) Tactile hairs and the adjustment of body height in wandering spiders: behavior, leg reflexes, and afferent projections in the leg ganglia. J Comp Physiol A 162:611–621

Eckweiler W, Hammer K, Seyfarth E-A (1989) Long, smooth hair sensilla on the spider leg coxa: sensory physiology, central projection pattern, and proprioceptive function (Arachnida, Araneida). Zoomorphology 109:97–102

Foelix RF (1996) Biology of spiders. Oxford University Press, Oxford

Foelix RF, Choms A (1979) Fine structure of a spider joint receptor and associated synapses. Eur J Cell Biol 19:149–159

French AS, Wong RKS (1976) The responses of trochanteral hair plate sensilla in the cockroach to periodic and random displacements. Biol Cybern 22:33–38

Harris DJ, Mill PJ (1977) Observations on the leg receptors of *Ciniflo* (Araneida: Dictynidae) I. External mechanoreceptors. J Comp Physiol 119:37–54

Humphrey JAC, Barth FG (2008) Medium flow-sensing hairs: biomechanics and models. In: Casas J, Simpson S (eds) Insect mechanics and control. Advances in insect physiology, vol 34. Elsevier, Amsterdam, pp 1–80

Keyserling E (1877) Über amerikanische Spinnenarten der Unterordnung Citigradae. Verh Zool-Bot Ges Wien 26:609–708

Kuenzi F, Burrows M (1995) Central connections of sensory neurones from a hair plate proprioceptor in the thoraco-coxal joint of the locust. J Exp Biol 198:1589–1601

McConney ME, Schaber CF, Julian MD, Eberhardt WC, Humphrey JAC, Barth FG, Tsukruk VV (2009) Surface force spectroscopic point load measurements and viscoelastic modelling of the micromechanical properties of air flow sensitive hairs of a spider (*Cupiennius salei*). J R Soc Interface 4:681–694

Mill PJ, Harris DJ (1977) Observations on the leg receptors of *Ciniflo* (Araneida: Dictynidae) III. Proprioceptors. J Comp Physiol 119:63–72

Newland PL, Watkins B, Emptage NJ, Nagayama T (1995) The structure, response properties, and development of a hair plate on the mesothoracic leg of the locust. J Exp Biol 198:2397–2404

Ogawa H, Kawakami Z, Yamaguchi T (2011) Proprioceptors involved in stinging response of the honeybee, *Apis mellifera*. J Insect Physiol 57:1358–1367

Paulk A, Gilbert C (2006) Proprioceptive encoding of head position in the black soldier fly, *Hermetia illucens* (L.) (Stratiomyidae). J Exp Biol 209:3913–3924

Poteser M, Pabst MA, Kral K (1998) Proprioceptive contribution to distance estimation by motion parallax in a praying mantid. J Exp Biol 201:1483–1491

Pringle JWS (1938) Proprioception in insects III. The function of the hair sensilla at the joints. J Exp Biol 15:467–473

Rathmayer W (1967) Elektrophysiologische Untersuchungen an Proprioreceptoren im Bein einer Vogelspinne (*Eurypelma hentzi* Chamb.). Z vergl Physiol 54:438–454

Schaber CF, Gorb SN, Barth FG (2012) Force transformation in spider strain sensors: white light interferometry. J R Soc Interface 9:1254–1264

Schmid A (1998) Different functions of different eye types in the spider *Cupiennius salei*. J Exp Biol 201:221–225

Seyfarth E-A (1985) Spider proprioception: receptors, reflexes and control of locomotion. In: Barth FG (ed) Neurobiology of arachnids. Springer, New York, pp 230–248

Seyfarth E-A (2002) Tactile body raising: neuronal correlates of a `simple´ behavior in spiders. In: Toft S, Scharff N (eds) European arachnology 2000. Aarhus University Press, Aarhus, pp 19–32

Seyfarth E-A, Pflüger HJ (1984) Proprioceptor distribution and control of a muscle reflex in the tibia of spider legs. J Neurobiol 15:365–374

Seyfarth E-A, Gnatzy W, Hammer K (1990) Coxal hair plates in spiders: physiology, fine structure, and specific central projections. J Comp Physiol A 166:633–642

Speck-Hergenröder J, Barth FG (1988) Vibration sensitive hairs on the spider leg. Experientia (Basel) 44:13–14

Vedel JP (1986) Morphology and physiology of a hair plate sensory organ located on the antenna of the rock lobster *Palinurus vulgaris*. J Neurobiol 17:65–76

Wendler G (1964) Laufen und Stehen der Stabheuschrecke *Carausius morosus*: Sinnesborstenfelder in den Beingelenken als Glieder von Regelkreisen. Z Vergl Physiol 48:198–250

Wong RKS, Pearson KG (1976) Properties of the trochanteral hair plate and its function in the control of walking in the cockroach. J Exp Biol 64:233–249